PHYSICAL REVIEW B VOLUME 29, NUMBER 12 15 JUNE 1984

Transport properties of *n*-type metalorganic chemical-vapor-deposited $Al_xGa_{1-x}As$ ($0 \leq x \leq 0.6$)

P. K. Bhattacharya* and U. Das*
Department of Electrical and Computer Engineering, Oregon State University, Corvallis, Oregon 97331

M. J. Ludowise
Corporate Solid State Laboratory, Varian Associates, Inc., Palo Alto, California 94303
(Received 31 October 1983)

Temperature-dependent measurements in the range $20 \leq T \leq 600$ K have been made on undoped and Si-doped metalorganic chemical-vapor-deposition—grown $Al_xGa_{1-x}As$ ($0 \leq x \leq 0.6$) on GaAs. Data obtained from Hall and high-field measurements with the use of the probe technique have been analyzed. The transport parameters in the samples have been obtained from analysis of data and the relative importance of the various scattering mechanisms in different composition ranges have been elucidated. It is found that space-charge scattering plays an important role in limiting electron mobility at 300 K for $0 < x \leq 0.3$, and intervalley scattering plays the dominant role in the composition range $0.3 \leq x \leq 0.5$. Donor levels, with their activation energy E_D increasing with x up to 0.133 eV at $x = 0.35$, are present in the undoped samples. The dominant donor level in the Si-doped samples also exhibits a similar trend, with $E_D = 0.095$ eV for $x = 0.35$. High values of drift velocity in samples with $x \geq 0.4$ at 300 K and similar features observed in some samples with $x < 0.4$ at high temperatures have been attributed to electron transfer from the substrate to the epitaxial layers.

I. INTRODUCTION

The $Al_xGa_{1-x}As$ ternary alloys grown by metalorganic chemical-vapor deposition (MO-CVD) have emerged as important materials for the fabrication of heterojunction solar cells and other optoelectronic devices. It is therefore important to know their electrical and optical properties. The band structure of the alloys as a function of composition has now been fairly well established and has emerged from the work of several investigators on crystals grown by liquid-phase epitaxy (LPE), using different techniques.[1-6] The alloys have a direct band gap for $0 \leq x \leq 0.43$, where the Γ conduction minima are lowest in energy. In addition, the L conduction minima crosses over the X minima at $x = 0.37$ and the Γ minima at $x = 0.47$. The energy position of the various conduction minima in the alloys at 300 K are shown in Fig. 1. The continuously changing band structure with composition has a marked influence on the material properties. Yang[7] has reported transport data taken by Hall measurements of alloys grown by MO-CVD, and Stringfellow and Künzel[8,9] have reported analysis of electron mobility data.

In this paper we report the results obtained from a detailed investigation of the transport properties of high-purity undoped and Si-doped n-type MO-CVD $Al_xGa_{1-x}As$ alloys. This includes measurement of electron velocities at high electron fields and an identification of scattering mechanisms in relatively pure crystals. Relevant comparisons have been made with similar high-purity crystals grown by LPE. The ionization energy of Si donors for $0.18 \leq x \leq 0.35$ has been determined from an accurate analysis of Hall-effect data.

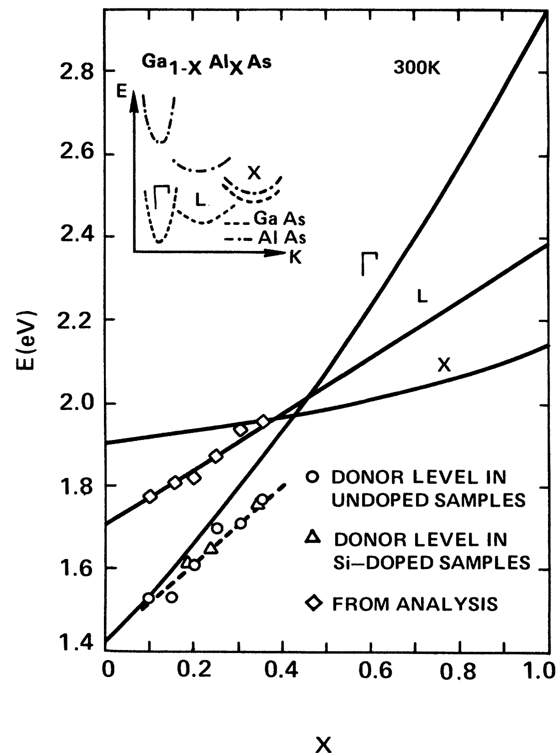

FIG. 1. Conduction-band structure in $Al_xGa_{1-x}As$ as determined from earlier work (see the text). Data points for the energy position of the L minima and the donor levels were determined in this study.

 ©1984 The American Physical Society

II. CRYSTAL GROWTH AND DEVICE FABRICATION

Undoped and Si-doped $Al_xGa_{1-x}As$ layers, 5—10 μm thick and with $0 \leq x \leq 0.6$, were grown on (100) GaAs:Cr substrates at 750 °C with a V/III ratio of ~ 10. Some of the layers studied were grown at 690 °C with a V/III ratio of 20. The alloy compositions were determined from the peak energy of photoluminescence at 1.9 and 4.4 K. Symmetrical samples with alloyed Ag-Sn contacts were made for the Hall measurements. These measurements were typically performed in the temperature range 20—600 K with a magnetic field of 0.4 T.

Measurements of the electron velocity in high electric fields were made in *H*-shaped planar Gunn-effect devices. These devices of varying dimensions were delineated by photolithography on the epitaxial layers. Alloyed Ag-Sn Ohmic contacts were formed at the large-area ends of the bridge. The potential distribution across the device was measured by a high-impedence Ni probe and the current flowing through the device was measured at the same time. The measurements were done with a pulsed-[$\sim$40-ns, (100—200)-Hz] voltage supply to avoid resistive heating of the sample. The velocity-field characteristics were derived from the measured data by considering the material and circuit parameters.

III. EXPERIMENTAL RESULTS

We consider the high-field transport properties first. A typical current-field profile in the prethreshold region measured in a device made from a direct-band-gap sample is shown in Fig. 2. Velocity-field characteristics are derived from such characteristics by normalizing the slopes at the low-field end of the curves to drift mobilities. It should be remembered that the ratio of the Hall-to-drift mobilities, μ_H/μ_d, is dependent on composition in the $Al_xGa_{1-x}As$ alloy system due to band crossover and a three-conduction-band model must be considered in calculating μ_H and n_H. Values for μ_H/μ_d calculated by Sugeta *et al.*[10] with the use of such a model are used in this study. The computed velocity-field characteristics for some alloy compositions are shown in Fig. 3. The point of interest is the higher velocities measured in the sample with $x = 0.4$ compared to those measured for $x = 0.32$ or those in indirect-band-gap crystals with $x \simeq 0.4$ grown by LPE.[10]

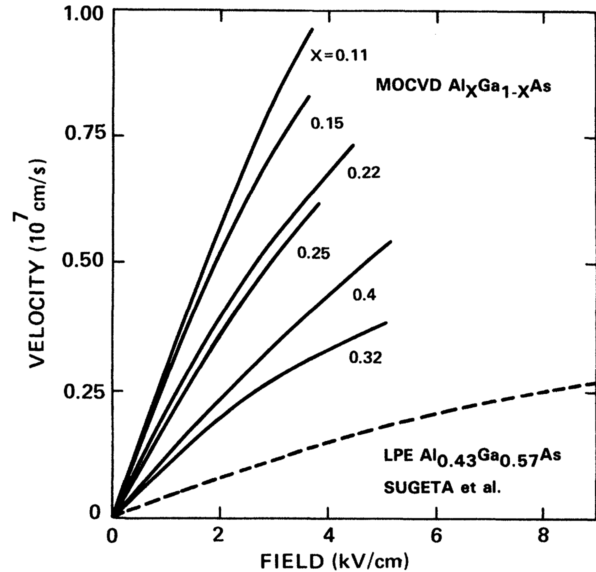

FIG. 3. Velocity-field characteristics of electron in MO-CVD $Al_xGa_{1-x}As$ with $0 \leq x \leq 0.4$.

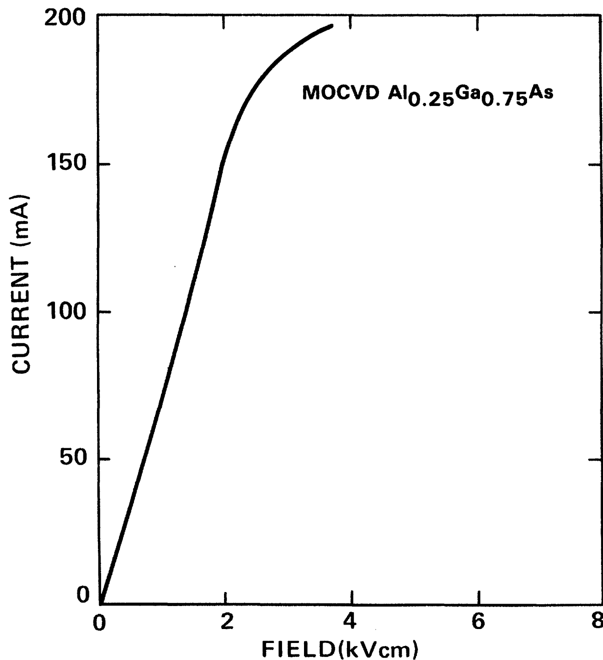

FIG. 2. Current-field characteristics in $Al_{0.25}Ga_{0.75}As$. Applied voltage pulses are of 40-ns duration.

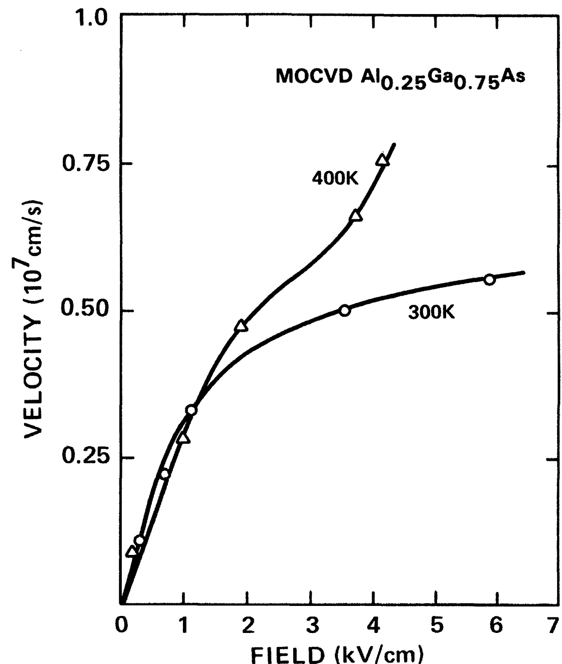

FIG. 4. Velocity-field characteristics of electrons in $Al_{0.25}Ga_{0.75}As$ at 300 and 400 K.

The measurements were repeated at temperatures above room temperature with a sample having $x=0.25$. The data are shown in Fig. 4. It is seen that at very low fields, the mobility at 400 K is smaller than that at room temperature. This lowering is caused by increasing phonon scattering at the higher temperatures. At higher fields, there is first a decrease and then at increase in the velocity at a slower rate.

Figure 5 is a plot of the variation of μ_H at room temperature as a function of alloying composition in crystals which have very similar background impurity concentrations. The observed variation can be qualitatively explained as follows. In the region $0 \leq x \leq 0.30$, the observed decrease in mobility can almost be totally explained by the increased polar-optical-phonon scattering which is the dominant scattering mechanism around 300 K. The increase in scattering is, in turn, due to the increase in the effective mass m_Γ^* of the electrons at progressively higher energy in the Γ valley. In the band-crossover region ($0.3 < x \leq 0.5$), significant carrier transfer to the subsidiary minima takes place, causing a sharp fall in the mobility value. For $x \geq 0.6$, the electrons reside mainly in the X minima, and the measured low values of mobility are indicative of the high electron effective mass in these minima. A minimum in mobility value usually occurs at $x \simeq 0.45$. This is due to a combination of intervalley, space-charge, and alloy scattering mechanisms. In comparison with electron mobility values in LPE $Al_xGa_{1-x}As$ with identical compositions and similar net donor densities, we find that the measured mobilities in MO-CVD $Al_xGa_{1-x}As$ are less by a factor of 2.0. At the same time, the photoluminescence intensities in the MO-CVD crystals are also slightly less than in LPE crystals. These facts indicate higher compensation in the MO-CVD materials studied here compared to LPE-grown crystals.

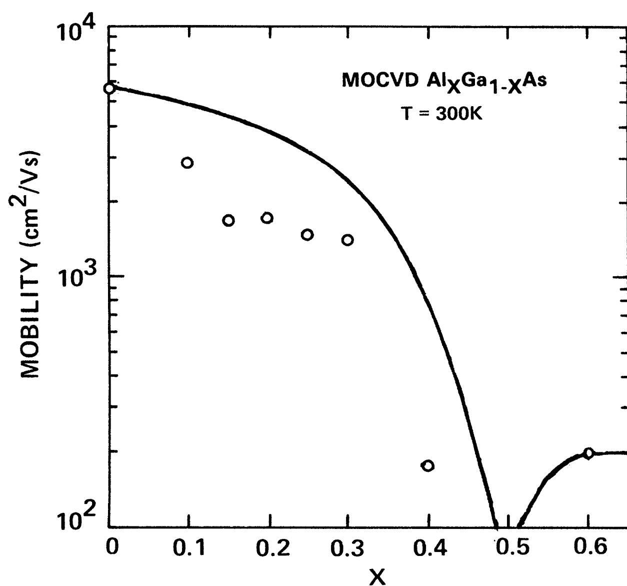

FIG. 5. Measured variation of Hall mobility with composition at 300 K in undoped MO-CVD $Al_xGa_{1-x}As$. Solid line indicates the mobilities calculated by Saxena (Ref. 17) from fitting of the data obtained from LPE-grown samples.

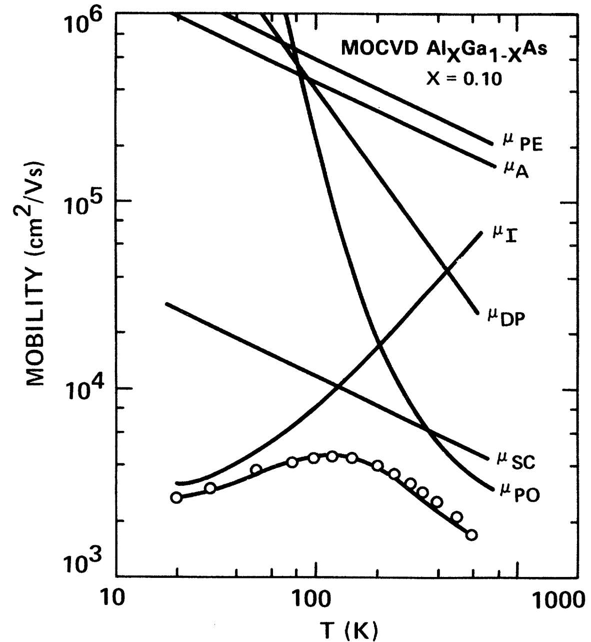

FIG. 6. Variation of Hall mobility with temperature in undoped MO-CVD $Al_{0.1}Ga_{0.9}As$. Solid line with the data indicates the calculated variation.

Hall mobilities in the samples were also measured in the temperature range 20—600 K. Typical variations of μ_H with T in two samples with $x=0.10$ and 0.25 are shown in Figs. 6 and 7, respectively. The relevant scattering mechanisms responsible for the measured mobility variations and analysis of the data will be discussed in detail in the next section.

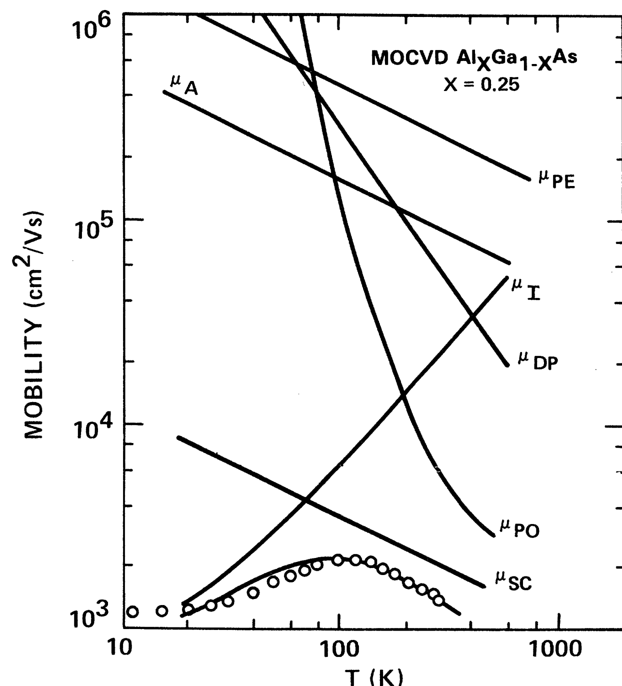

FIG. 7. Variation of Hall mobility with temperature in undoped MO-CVD $Al_{0.25}Ga_{0.75}As$. Solid line with the data indicates the calculated variation.

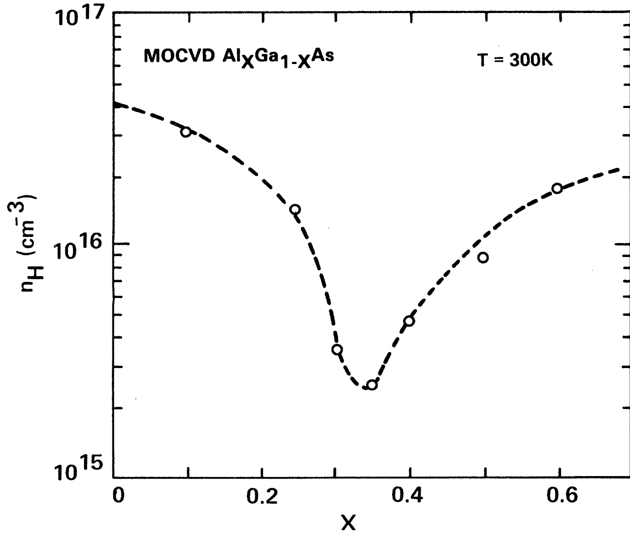

FIG. 8. Measured variation of Hall electron concentration with composition at 300 K in undoped MO-CVD $Al_xGa_{1-x}As$. Dashed line depicts the nature of variation.

Figure 8 shows the measured variation of the Hall-electron concentration, n_H, with alloy composition at room temperature. Data from a limited number of samples, grown under similar conditions, are presented here. The observed variation can be interpreted as follows. With increasing x, increasing numbers of carries transfer to the subsidiary minima which have high density of states and low mobilities, resulting in a lowered value of n_H. The minimum occurs at a composition slightly below the Γ-X crossover composition. As x increases further, most of the electrons reside in the X minima, and n_H increases to the value of the electron concentration in these minima.

The variation of n_H with temperatures in the range 300—600 K in three undoped samples with $x=0.1$, 0.2, and 0.3 is depicted in Fig. 9. The decrease in electron concentration with an increase of temperature is due to carrier transfer to the subsidiary minima. The variation

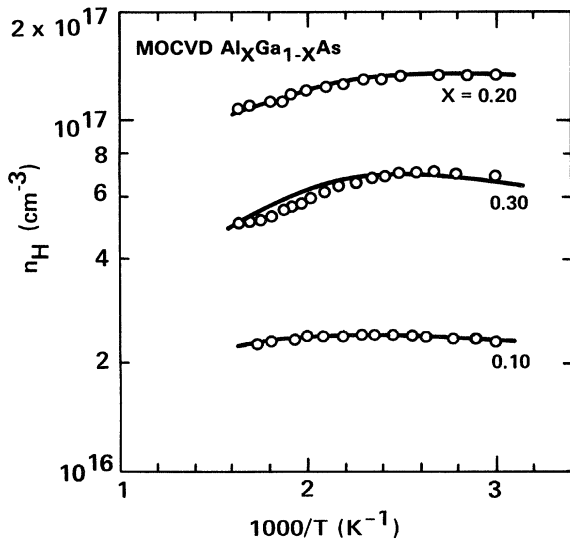

FIG. 9. Measured and calculated variations of Hall electron concentration with temperature in undoped $Al_xGa_{1-x}As$ samples.

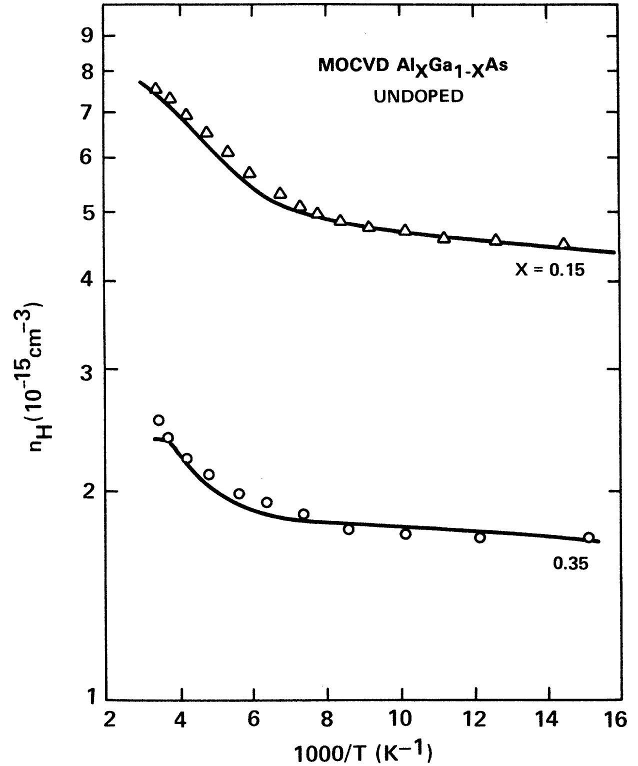

FIG. 10. Measured and calculated variations of Hall electron concentration with temperature in undoped $Al_xGa_{1-x}As$ samples.

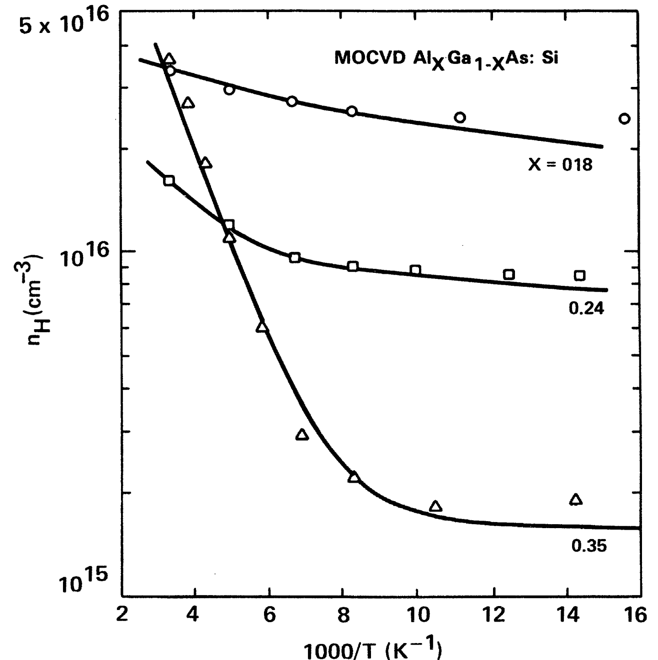

FIG. 11. Measured and calculated variations of Hall electron concentration with temperature in Si-doped $Al_xGa_{1-x}As$ samples.

of n_H with temperature for undoped and Si-doped samples of different compositions is depicted in Figs. 10 and 11, respectively.

IV. ANALYSIS AND DISCUSSION

To analyze mobility data, the following assumptions are usually made: (a) each scattering process has a characteristic relaxation time $\tau(E)$ where E is the electron energy in k_BT; (b) the electrons are scattered in a parabolic band; and (c) the various scattering mechanisms are independent of each other. It should be remembered that the last assumption may not be strictly valid, since an electron-phonon interaction could take place while the electron's motion is influenced by the potential of an ionized impurity. Also, a true relaxation time cannot strictly be defined for electron scattering by polar-optical modes.[11] In spite of these facts, the above assumptions are valid to a large extent and give a good insight into scattering processes in III-V semiconductors.

The Γ-L-X conduction-band structure as a function of alloy composition plays an important role in determining the mobility. In the composition range $0 \le x \le 0.3$, the transport properties are primarily determined by the electrons in the Γ minimum. The effects of the L and X minima may be neglected. Similarly, in crystals with $0.6 \le x \le 1.0$, the X minima plays the major role. In the intermediate band-crossover composition range, $0.3 \le x \le 0.6$, the effects of Γ, L, and X minima must be considered. Considering three-valley conduction, n_H and μ_H can be expressed as

$$n_H = n_\Gamma \left[1 + \frac{n_X}{n_\Gamma}\frac{\mu_X}{\mu_\Gamma} + \frac{n_L}{n_\Gamma}\frac{\mu_L}{\mu_\Gamma}\right] \Big/ \left[1 + \frac{n_X}{n_\Gamma}\left[\frac{\mu_X}{\mu_\Gamma}\right]^2 + \frac{n_L}{n_\Gamma}\left[\frac{\mu_L}{\mu_\Gamma}\right]^2\right] \quad (1)$$

and

$$\mu_H = \mu_\Gamma \left[1 + \frac{n_X}{n_\Gamma}\left[\frac{\mu_X}{\mu_\Gamma}\right]^2 + \frac{n_L}{n_\Gamma}\left[\frac{\mu_L}{\mu_\Gamma}\right]^2\right] \Big/ \left[1 + \frac{n_X}{n_\Gamma}\frac{\mu_X}{\mu_\Gamma} + \frac{n_L}{n_\Gamma}\frac{\mu_L}{\mu_\Gamma}\right] . \quad (2)$$

Assuming that Boltzmann statistics are valid for the electron concentrations in the crystals studied, the following approximate relations are also valid:

$$n_\Gamma = N_c^\Gamma \exp(E_F/k_BT) ,$$
$$\frac{n_{L,X}}{n_\Gamma} = \left[\frac{m^d_{L,X}}{m_\Gamma}\right]^{3/2} \exp\left[-\frac{\Delta E_{\Gamma L,\Gamma X}}{k_BT}\right] , \quad (3)$$

where $(n,m^d,\mu)_{\Gamma,L,X}$ are the transport parameters in the different conduction valleys and $\Delta E_{\Gamma L}$ and $\Delta E_{\Gamma X}$ are the Γ-L and Γ-X intervalley seperations. m^d is the density-of-states effective mass.

The processes which must be considered for deriving a reasonable theoretical estimate of carrier mobility are, polar-optical-phonon scattering, deformation-potential scattering, piezoelectric scattering, ionized impurity scattering, space-charge scattering, alloy scattering, and equivalent and nonequivalent intervalley scattering. In what follows, some of the scattering mechanisms and the relevant parameters are discussed in more detail.

The temperature dependence of mobility limited by polar-optical- (PO-) phonon scattering is calculated from the analysis of Fortini[12] as

$$\mu_{PO} = 25.44 \frac{\epsilon_s \epsilon_d [\exp(\Theta/T) - 1]}{(\epsilon_s - \epsilon_d)(m^*/m_0)^{3/2}\Theta} G\left[\frac{\Theta}{T}\right] T^{1/2} , \quad (4)$$

where ϵ_s and ϵ_d are the static and high-frequency dielectric constants and Θ is the optical-phonon temperature. $G(\Theta/t)$ is an integral function which has been determined by Fortini.[12] The infrared reflection spectra of $Al_xGa_{1-x}As$ at the Γ point contain two branches, related to GaAs and AlAs.[13] The term $\Theta/[\exp(\Theta/T) - 1]$ is the average phonon energy per mode, $\bar{E}$, which can be expressed as

$$\bar{E} = x\bar{E}_{AlAs} + (1-x)\bar{E}_{GaAs} . \quad (5)$$

Similarly, the integral function may be interpolated as

$$G(\Theta/T) = xG(\Theta/T)_{AlAs} + (1-x)G(\Theta/T)_{GaAs} . \quad (6)$$

The LO-phonon temperature in GaAs at the X point is 345 K (Ref. 14), and its value of AlAs is taken to be the same as that in GaP (Ref. 15), namely 580 K. A linear interpolation between the two values is used to calculate $\Theta^X_{LO}(x)$. The value of Θ^L_{LO} is not known for GaAs or AlAs.

The relaxation time due to alloy scattering has been determined by Hauser *et al.*[16] The temperature dependence of mobility can be expressed as

$$\mu_A = \frac{52.8T^{-1/2}}{(m^*/m_0)^{5/2}x(1-x)(\Delta U)^2} , \quad (7)$$

where the alloy scattering potential ΔU is given by[17]

$$\Delta U = 0.3 + 0.011x . \quad (8)$$

From the space-charge (SC) scattering formulation of Weisberg,[18] the temperature dependence of mobility can be expressed as

$$\mu_{SC} = \frac{3.2 \times 10^9 T^{-1/2}}{(m^*/m_0)^{1/2}(N_sA)} , \quad (9)$$

where N_s and A are the concentration and area of scattering center, respectively. It should be noted that the mobilities limited by alloy and space-charge scattering mechanisms have an identical temperature dependence.

The scattering rate from a k state in the i valley to a state in the j valley has been derived by Fawcett *et al.*[19] With the use of this expression and the approximation $E \cong \frac{3}{2}k_BT$, the mobility limited by nonequivalent intervalley (IV) scattering can be expressed as

$$\mu_{\rm IV}=\frac{8\sqrt{\pi}}{3(m_j^*)^{5/2}}\frac{q\hbar^2\rho\sqrt{k\Theta}}{\sqrt{3}N_jD_{ij^2}}\left[\left[\left[\frac{T}{\Theta}+\frac{2}{3}+\frac{\Delta E_{ij}}{k_BT}\right]^{1/2}\Big/(e^{\Theta/T}-1)\right]+\left\{\left[\frac{T}{\Theta}-\left[\frac{2}{3}+\frac{\Delta E_{ij}}{k_BT}\right]\right]^{1/2}\Big/(1-e^{-\Theta/T})\right\}\right]^{-1}$$

$$\text{for } \frac{T}{\Theta}\geq\frac{2}{3}+\frac{\Delta E_{ij}}{k_BT}\,. \qquad (10)$$

In this expression ρ is the material density. The last term on the right-hand side is 0 for $T/\Theta<\frac{2}{3}+\Delta E_{ij}/k_BT$. Here, N_j is the number of equivalent minima and m_j^* is the mass in a single minimum. ΔE_{ij} is the intervalley separation. $(N_j^{2/3}m_j^*)$ is the combined density-of-states mass for the j valley. In the case of equivalent intervalley scattering, the above expression is applicable when N_j is changed to (N_j-1) and $\Delta E_{ij}=0$. It has been found that intervalley scattering involving the Γ minimum has very little influence in determining electron mobility in the $Al_xGa_{1-x}As$ alloys and therefore the only scatterings to be considered in the range $0.3<x\leq1.0$ involve the L and X minima. According to the selection rules of Birman *et al.*,[20] $\Theta=\Theta_{\rm LO}^X$ can be assumed. Values of the coupling coefficients D_{XX} and D_{LX} have been taken from Saxena and Gurumurthy,[21] and these values agree reasonably well with earlier published data.[22]

One of the most crucial parameters needed for the calculation of mobilities in the various minima for various values of x is the electron effective mass. Since the energy of the X minima remains almost invariant with x, a constant value of the density-of-state effective mass $m_X^*=0.35m_0$ in a single minimum is used,[23] assuming three equivalent minima. The variation of the effective mass in the Γ valley is obtained from $\vec{k}\cdot\vec{p}$ theory as[24]

$$\left[\frac{m_0}{m_\Gamma^*}\right]=1+7.51\left[\frac{2}{E_\Gamma}+\frac{1}{E_\Gamma+0.341}\right], \qquad (11)$$

where E_Γ is the energy of the Γ minimum. Similarly, using $\vec{k}\cdot\vec{p}$ theory to calculate the transverse effective mass m_t in the L minima and knowing that the longitudinal effective mass $m_l=1.9m_0$, it has been found that[21]

$$m_L^*=N^{2/3}m_t^{2/3}m_l^{1/3}\simeq(0.55+0.76x)m_0 \quad (N=4)\,. \qquad (12)$$

The other parameter intimately related to the band structure is the acoustic deformation potential E_1. In this study, we have taken $E_1^\Gamma=8.6$ eV, as determined in GaAs, to be constant throughout the composition range. Saxena and Gurumurthy[21] have determined E_1^X from analysis of data recorded at 300 K and the value of this parameter varies from 5.1 eV at $x=0$ to 13.0 eV at $x=1$. The latter value agrees well with earlier data.[23] The value of E_1^L is unknown. The values of parameters such as dielectric constants ϵ density ρ, longitudinal velocity of sound in the medium μ_l, and the elastic constants c_t and c_l, in the alloys have been determined by linear interpolation between their values in GaAs and AlAs. Some of the more important parameters and their values used in this study are listed in Table I. The temperature dependence of the band minima energies are also taken into account by using the Varshni equation.[25]

In order to estimate the theoretical mobility at each temperature, it is necessary to calculate μ_Γ, μ_L, and μ_X limited by the various scattering mechanisms using Mattheson's rule. The Hall mobility is then calculated by using Eq. (2). For $0\leq x\leq0.3$, it may be assumed that $\mu_H\simeq\mu_\Gamma$ and for $x>0.6$, $\mu_H\simeq\mu_X$. In the region $0.3<x<0.6$, the mobilities in all three conduction minima must be taken into account. This poses a problem since the material parameters for the L minima are largely unknown. We have circumvented this by assuming $\mu_\Gamma/\mu_L\simeq8.5$, as determined by Sagar[26] and Kosicki *et al.*[27] from hydrostatic pressure experiments on GaSb. We have also assumed this ratio to remain constant with temperature. The calculated variations of μ_Γ, μ_X, and μ in $Al_{0.4}Ga_{0.6}As$ are shown in Fig. 12. The calculated

TABLE I. Values of material parameters used for analysis of Hall mobility data.

Parameters	GaAs $x=0$	AlAs $x=1$
$\Theta_{\rm LO}^X$ (K)	345	580
$\Theta_{\rm LO}^\Gamma$ (K)	420	
ϵ_s	12.9	10.06
ϵ_∞	10.9	8.16
ρ (g/cm^3)	5.37	3.60
u_l (km/s)	5.24	5.50
E_1^Γ, E_1^X (eV)	8.6	13.0
e_{14} (C/m^2)	0.16	0.16
c_t (dyn/cm^2)	4.87×10^{11}	4.93×10^{11}
c_l (dyn/cm^2)	1.404×10^{12}	1.422×10^{12}
D_{XX} (eV/cm)	3.37×10^8	1.47×10^9

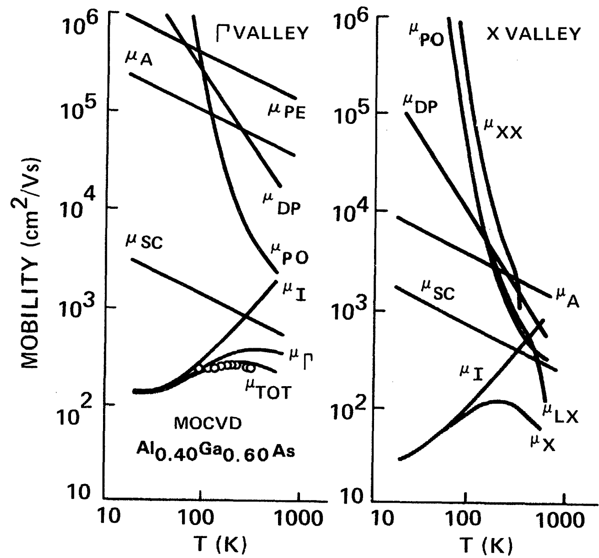

FIG. 12. Electron mobilities limited by the different relevant scattering mechanisms in Γ and X minima in $Al_{0.4}Ga_{0.6}As$. Solid line alongside the data indicates the total calculated mobility $\mu_{\rm TOT}$.

TABLE II. Characteristics of undoped and Si-doped MO-CVD $Al_xGa_{1-x}As$ obtained from analysis of Hall data.

Samples	n	N_D ($\times 10^{16}$) (cm^{-3})	N_A ($\times 10^{16}$) (cm^{-3})	Compensation ratio N_D+N_A/N_D-N_A	N_sA (cm^{-1})($\times 10^5$) from analysis	N_sA (cm^{-1})($\times 10^5$) from Eq. (13)
1	0.10	3.8	2.7	5.9	1.2	0.7
2	0.15	1.0	0.3	1.9	2.4	1.0
3	0.20	4.3	3.6	11.3	1.6	1.3
4	0.25	1.8	0.1	1.1	3.0	1.6
5	0.30	0.54	0.04	1.2	2.6	2.0
6[a]	0.18	9.1	8.0	15.5	2.7	0.7
7[a]	0.24	8.3	7.3	15.6	2.0	1.3
8[a]	0.35	34.0	33.3	67.0	2.4	2.0

[a]Si-doped samples.

mobilities for $x=0.10$ and 0.25 are indicated by the solid lines in Figs. 6 and 7, respectively.

Mobilities for other compositions in the range $0<x\leq 0.4$ were calculated by the procedure outlined above. Values of N_SA, N_D, and N_A required to obtain good agreement of the calculated mobilities with the data are listed in Table II. Also listed are values of N_sA calculated by the empirical formulation of Kaneko *et al.*[28] and Stringfellow[8] as follows:

$$N_sA = 5\times 10^3 + 6.3\times 10^5 x \ (cm^{-1}) . \quad (13)$$

The agreement is fair. Slightly higher values derived by us may reflect the influence of deep levels in the samples. The ratio μ_A/μ_{SC} at 300 K calculated by us from fitting of the data is shown in Fig. 13 for a limited composition range. It is clear that the relative importance of alloy scattering, compared to scattering by space charge, increases with increasing x.

The calculated mobilities limited by alloy, space-charge, and intervalley scattering in the Γ and X minima for a limited composition range near band crossover are depicted in Fig. 14. The data points indicate the calculated values obtained by fitting to the experimental results.

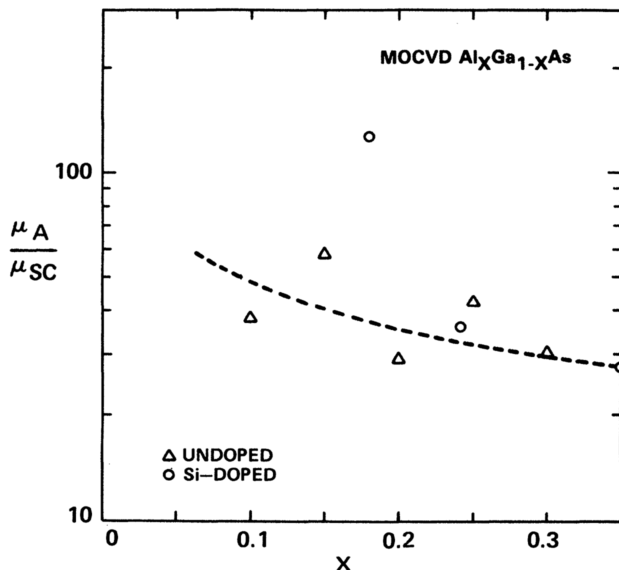

FIG. 13. Ratio of mobilities limited by alloy and space-charge scattering. Symbols represent values derived from analysis of mobility data. Dashed line indicates a mean trend.

The charge-neutrality condition, assuming three-band conduction, can be expressed as

$$\sum_i N_{Di} - N_A = \sum_i n_{di} + n_\Gamma + n_L + n_X , \quad (14)$$

where N_{Di} and N_A are the total density of donor (ith lev-

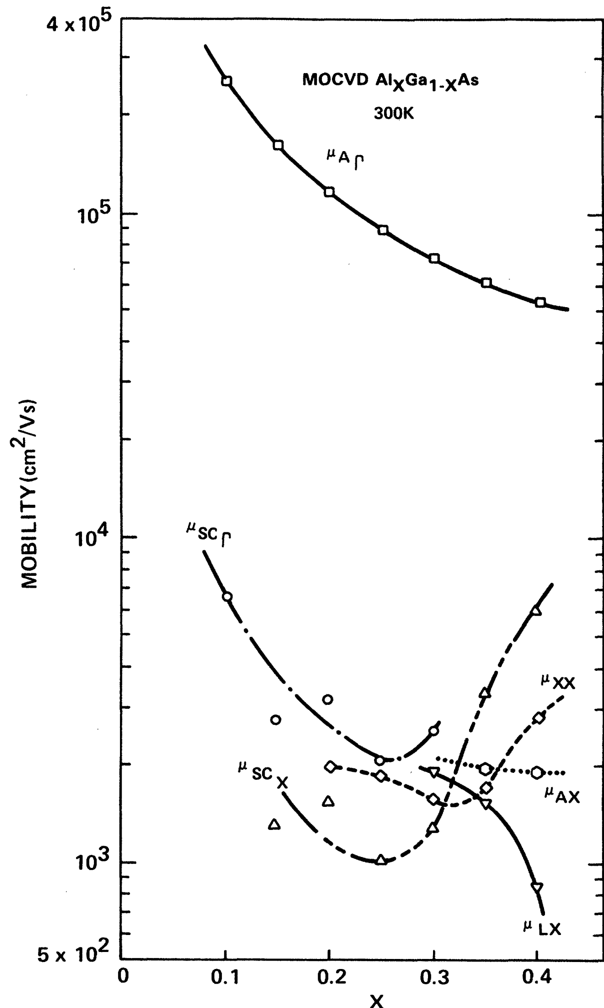

FIG. 14. Mobilities in Γ and X valleys limited by alloy, space-charge, and intervalley scattering in $Al_xGa_{1-x}As$. Symbols represent values derived from analysis of mobility data. Curves passing through the symbols have been drawn to depict the nature of variation for each scattering mechanism.

el) and acceptor impurities and n_{di} is the density of occupied donors (ith level). Combined with Eq. (3), Eq. (14) can be solved fairly accurately to determine the various densities, Fermi energy, and intervalley separations. Values of n_H calculated for the samples of Fig. 9 are shown by the solid lines alongside the data. Analysis of the data recorded at higher temperatures gives the value of $\Delta E_{\Gamma L}$ for $0 \leq x < 0.3$. These calculated values are shown in Fig. 1 and the agreement with previous data is excellent. Analysis of data similar to those shown in Figs. 10 and 11 gives the value of donor ionization energy and donor and acceptor concentrations. The values of these concentrations are in good agreement with the corresponding values derived from analysis of the mobility data. We find that there is a donor level in the undoped samples whose ionization energy increases from 0.025 to 0.113 eV in the composition range $0.15 \leq x \leq 0.35$. Ionization energies of Si donors in the Si-doped samples were obtained from analysis of the data of Fig. 11 and are 0.022, 0.077, and 0.095 eV, respectively, for $x = 0.18$, 0.24, and 0.35. The value of the donor ionization energy in Si-doped $Al_{0.24}Ga_{0.76}As$ is in good agreement with the value of 0.065 eV in a crystal with similar composition estimated by Fischer *et al.*[29] from photoluminescence pair-transition data. Similar to several other donor species in LPE materials[5,30,31] the activation energy of the donors in MO-CVD samples also increases with increasing x. The increase can be explained by considering the interaction of the Γ, L, and X wave functions near the band-crossover region. The increasing donor energies would be undesirable for device applications.

An inflexion similar to that observed in the velocity-field characteristics of $Al_{0.25}Ga_{0.75}As$ at high temperatures has also been observed earlier by us in GaAs-$Al_{0.4}Ga_{0.6}As$ modulation-doped heterostructures[32] in which the effect was attributed to real-space electron transfer[33] from GaAs to $Al_xGa_{1-x}As$ at high fields. In the epitaxial layer with $x = 0.25$ grown directly on a semi-insulating substrate, the velocities measured at room temperature are a combination of those for electrons in the ternary layer and some which have transferred to the GaAs substrate. The major contribution to the velocity is, however, from the electrons in the ternary layer. At room temperature, the electrons in GaAs cannot gain sufficient energy to surmount the heterostructure barrier and be emitted into the ternary layer. It is quite probable that $\vec{k}$-space transfer of electrons from the Γ to the L valleys in $Al_{0.35}Ga_{0.75}As$ would occur before real-space transfer, thereby causing a velocity saturation. At 400 K, the electrons in GaAs gain an extra amount of energy and therefore real-space transfer is possible. From the analysis of the data presented in Fig. 9, we know that significant $\vec{k}$-space transfer starts only at $T \geq 500$ K. However, the amount of inflexion observed here is too large and it should be observed below the 300-K characteristic. These anomalous features indicate that other unidentified effects may also be responsible for the observed data. By involving transfer doping, the observed high-drift velocities for $x \geq 0.4$ can be explained. Once again, the measured value reflects a combination of the velocity of electrons at $Al_xGa_{1-x}As$ and in GaAs, but now the velocity of electrons in the GaAs is higher and contributes primarily to the measured value.

V. CONCLUSION

A detailed study of the transport properties in undoped and Si-doped MO-CVD $Al_xGa_{1-x}As$ $(0 < x \leq 0.6)$ has been made. Data obtained from Hall measurements in the temperature range $20 \leq T \leq 600$ K have been analyzed by considering the relevant scattering mechanisms. The functions of alloy, intervalley, and space-charge scatterings have been investigated in detail. It is found that the sharp fall in mobility at the band-crossover region is caused by equivalent and nonequivalent intervalley scattering. The variation of the measured Hall electron concentration with temperature has been analyzed using a three-valley conduction-band charge-neutrality model. The analysis yields the Γ-L intervalley separation for $0 < x \leq 0.3$, donor-level ionization energies, and donor- and acceptor-level concentrations. It is found that a donor level with $0.025 \leq E_D \leq 0.113$ eV is present in the undoped samples with $0.1 \leq x \leq 0.35$ and a donor level with $0.022 \leq E_D \leq 0.095$, eV possibly arising from Si impurities, is present in the Si-doped samples with $0.18 \leq x \leq 0.35$. The drift velocity of electrons in these alloys at high fields has been measured by a probe technique and anomalous behavior in the velocity-field characteristics at high x and high temperatures has been explained by involving modulation doping and real-space electron transfer effects.

ACKNOWLEDGMENTS

The authors acknowledge useful discussions with Professor J. S. Blakemore (Oregon Graduate Center), the continued support of Dr. R. L. Bell, and the technical support of S. Hikido (Varian). The work at Oregon State University has been supported by the Department of Energy, Office of Basic Energy Sciences, under Contract No. DE-AT06-81ER10939.

---

*Present address: Solid-state Electronics Laboratory, Department of Electrical and Computer Engineering, University of Michigan, Ann Arbor, MI 48109.

[1]C. A. Mead and W. G. Spitzer, Phys. Rev. Lett. 11, 358 (1963).

[2]H. C. Casey and M. B. Panish, J. Appl. Phys. 40, 4910 (1969).

[3]M. R. Lorenz, R. Chicotka, G. D. Pettit, and P. J. Dean, Solid State Commun. 8, 693 (1970).

[4]R. Dingle, R. A. Logan, and J. R. Arthur, in *Proceedings of the Sixth International Symposium on Gallium Arsenide and Related Compounds, Edinburgh,* edited by C. Hilsum (IOP, Bristol, 1977), p. 210.

[5]A. K. Saxena, Phys. Status. Solidi B 96, K77 (1979); Appl. Phys. Lett. 36, 79 (1980).

[6]P. K. Bhattacharya, A. Majerfeld, and A. K. Saxena, in *Proceedings of the Seventh International Symposium on Galli-*

um Arsenide and Related Compounds, St, Louis, edited by C. M. Wolfe (IOP, Bristol, 1979), p. 199.

[7]J. J. Yang, W. I. Simpson, and L. A. Moudy, J. Appl. Phys. 53, 771 (1982); Appl. Phys. Lett. 40, 244 (1982).

[8]G. B. Stringfellow, J. Appl. Phys. 50, 4178 (1979).

[9]G. B. Stringfellow and H. Künzel, J. Appl. Phys. 51, 3254 (1980).

[10]T. Sugeta, A. Majerfeld, A. K. Saxena, P. N. Robson, and G. Hill, *Proceedings of the Sixth Biennial Cornell Conference on Active Microwave Semiconductor Devices and Circuits* (Cornell University Press, Ithaca, 1977), p. 45.

[11]B. R. Nag, *Theory of Electrical Transport in Semiconductors* (Pergamon, Oxford, 1982), p. 187.

[12]A. Fortini, J. Appl. Phys. 41, 3121 (1970).

[13]M. Ilegems and G. L. Pearson, Phys. Rev. B 1, 1576 (1970).

[14]J. L. T. Waugh and G. Dolling, Phys. Rev. 132, 2410 (1963).

[15]D. L. Rode, Phys. Status Solidi B 53, 245 (1972).

[16]J. R. Hauser, M. A. Littlejohn, and T. H. Glisson, Appl. Phys. Lett. 28, 458 (1976).

[17]A. K. Saxena, Phys. Rev. B 24, 3295 (1981).

[18]L. R. Weisberg, J. Appl. Phys. 33, 1817 (1962).

[19]W. Fawcett, A. D. Boardman, and S. Swain, J. Phys. C 31, 1963 (1970).

[20]J. L. Birman, M. Lax, and R. Loudon, Phys. Rev. 145, 620 (1966).

[21]A. K. Saxena and K. S. Gurumurthy, J. Phys. Chem. Solids 43, 801 (1982).

[22]M. A. Littlejohn, J. R. Hauser, and T. H. Glisson, J. Appl. Phys. 48, 4587 (1977).

[23]A. S. Epstein, J. Phys. Chem. Solids 27, 1611 (1966).

[24]D. E. Aspnes, Phys. Rev. B 14, 5331 (1976).

[25]Y. P. Varshni, Physica (Utrecht) 39, 149 (1967).

[26]A. Sagar, Phys. Rev. 117, 93 (1960).

[27]B. B. Kosicki, A. Jayaraman, and W. Paul, Phys. Rev. 172, 764 (1968).

[28]K. Kaneko, M. Ayabe, and N. Watanabe, in *Proceedings of the Sixth International Symposium on Gallium Arsenide and Related Compounds,* Ref. 4, p. 216.

[29]P. Fischer, G. Kuhn, R. Bindemann, B. Rheinlander, and W. Horig, Krist. Tech. 8, 167 (1963).

[30]R. J. Nelson, Appl. Phys. Lett. 31, 351 (1977).

[31]A. J. SpringThorpe, F. D. King, and A. Becke, J. Electron Mater. 4, 101 (1975).

[32]T. Matsumoto, P. K. Bhattacharya, J. Darmawan, and M. J. Ludowise, Appl. Phys. Lett. 41, 1075 (1982).

[33]K. Hess, H. Morkoç, H. Shichijo, and B. G. Streetman, Appl. Phys. Lett. 35, 469 (1979).